

Simultaneous measurement of electro-optical and converse-piezoelectric coefficients of PMN-PT ceramics

Pingping Xiao,^{1,2} Xianping Wang,^{1,*} Jingjing Sun,¹ Meizhen Huang,¹ Xianfeng Chen,¹ and Zhuangqi Cao^{1,3}

¹Department of Physics, the State Key Laboratory on Fiber Optic Local Area Communication Networks and Advanced Optical Communication Systems, JiaoTong University, Shanghai, 200240, China

²College of Physics Science and Engineering technology, Yichun University, Yichun 336000, China

³zqcao@sjtu.edu.cn

*xpwangphysics@gmail.com

Abstract: A new scheme is proposed to measure the electro-optical (EO) and converse-piezoelectric (CPE) coefficients of the PMN-PT ceramics simultaneously, in which the PMN-PT ceramics acts as the guiding layer of a symmetrical metal-cladding waveguide. As the applied electric field exerts on the waveguide, the effective refractive index (RI) (or synchronous angle) can be effectively tuned from a selected mode to another adjacent mode owing to the high sensitivity and the small spacing of the ultra-high order modes. Subsequently, a correlation between EO and CPE coefficients is established. With this correlation and the measurement of the effective RI change to the applied voltage, the quadratic EO and CPE coefficients of PMN-PT ceramics are obtained simultaneously. The obtained results are further checked by fitting the variations of effective RI to a quadratic function. Our measurement method can be extended to a wide range of other materials.

©2012 Optical Society of America

OCIS codes: (120.4530) Optical constants; (130.2755) Glass waveguides; (160.2100) Electro-optical materials.

References and links

1. G. H. Haertling, "PLZT electro-optic materials and applications – a review," *Ferroelectrics* **75**(1), 25–55 (1987).
2. T. Tamura, K. Matsuura, H. Ashida, K. Kondo, and S. Otani, "Hysteresis variations of (Pb, La)(Zr, Ti)O₃ capacitors baked in a hydrogen atmosphere," *Appl. Phys. Lett.* **74**(22), 3395–3397 (1999).
3. H. Jiang, Y. K. Zou, Q. Chen, K. K. Li, R. Zhang, and Y. Wang, "Transparent electro-optic ceramics and devices," *Proc. SPIE* **5644**, 380–394 (2005).
4. S. W. Choi, T. R. Shrout, S. J. Jang, and A. S. Bhalla, "Morphotropic phase boundary in Pb(Mg_{1/3}Nb_{2/3})O₃-PbTiO₃ system," *Mater. Lett.* **8**(6-7), 253–255 (1989).
5. R. Zhang, B. Jiang, and W. Cao, "Elastic, piezoelectric, and dielectric properties of multidomain 0.67 Pb(Mg_{1/3}Nb_{2/3})O₃-0.33PbTiO₃ single crystals," *J. Appl. Phys.* **90**(7), 3471–3475 (2001).
6. B. Noheda, D. E. Cox, G. Shirane, J. Gao, and Z. G. Ye, "Phase diagram of the ferroelectric relaxor (1-x)PbMg_{1/3}Nb_{2/3}O₃-xPbTiO₃," *Phys. Rev. B* **66**(5), 054104 (2002).
7. O. Noblanc, P. Gaucher, and G. Calvarin, "Structural and dielectric studies of Pb(Mg_{1/3}Nb_{2/3})O₃-PbTiO₃ ferroelectric solid solutions around the morphotropic boundary," *J. Appl. Phys.* **79**(8), 4291–4297 (1996).
8. Y.-L. Lu, B. Gaynor, C. Hsu, G. Jin, M. Cronin-Golomb, F. Wang, J. Zhao, S.-Q. Wang, P. Yip, and A. J. Drehman, "Structural and electro-optic properties in lead magnesium niobate titanate thin films," *Appl. Phys. Lett.* **74**(20), 3038–3040 (1999).
9. Y. L. Lu and C. Gao, "Optical limiting in lead magnesium niobate-lead titanate multilayers," *Appl. Phys. Lett.* **92**(12), 121109 (2008).
10. B. C. Lim, P. B. Phua, W. J. Lai, and M. H. Hong, "Fast switchable electro-optic radial polarization retarder," *Opt. Lett.* **33**(9), 950–952 (2008).
11. Y. K. Zou, Q. S. Chen, R. Zhang, K. K. Li, and H. Jiang, "Low voltage, high repetition rate electro-optic Q-switch," in *Conference on Lasers and Electro-Optics/Quantum Electronics and Laser Science and Photonic Applications Systems Technologies*, Technical Digest (CD) (Optical Society of America, 2005), paper CTuZ5.
12. L. Qiao, Q. Ye, J. L. Gan, H. W. Cai, and R. H. Qu, "Optical characteristics of transparent PMNT ceramic and its application at high speed electro-optic switch," *Opt. Commun.* **284**(16-17), 3886–3890 (2011).

13. Y. T. Lin, B. Ren, X. Y. Zhao, D. Zhou, J. Chen, X. B. Li, H. Q. Xu, D. Lin, and H. S. Luo, "Large quadratic electro-optic properties of ferroelectric base $0.92\text{Pb}(\text{Mg}_{1/3}\text{Nb}_{2/3})\text{O}_3$ - 0.08PbTiO_3 single crystal," *J. Alloy. Comp.* **507**(2), 425–428 (2010).
14. C. J. He, W. W. Ge, X. Y. Zhao, H. Q. Xu, H. S. Luo, and Z. X. Zhou, "Wavelength dependence of electro-optic effect in tetragonal lead magnesium niobate lead titanate single crystals," *J. Appl. Phys.* **100**(11), 113119 (2006).
15. C. J. He, Z. X. Zhou, D. J. Liu, X. Y. Zhao, and H. S. Luo, "Photorefractive effect in relaxor ferroelectric $0.62\text{Pb}(\text{Mg}_{1/3}\text{Nb}_{2/3})\text{O}_3$ - 0.38PbTiO_3 single crystal," *Appl. Phys. Lett.* **89**(26), 261111 (2006).
16. S. E. Park and T. R. Shrout, "Ultrahigh strain and piezoelectric behavior in relaxor based ferroelectric single crystals," *J. Appl. Phys.* **82**(4), 1804–1811 (1997).
17. H. G. Li, Z. Q. Cao, H. F. Lu, and Q. S. Shen, "Free-space coupling of a light beam into a symmetrical metal-cladding optical waveguide," *Appl. Phys. Lett.* **83**(14), 2757–2759 (2003).
18. H. F. Lu, Z. Q. Cao, H. G. Li, and Q. S. Shen, "Study of ultrahigh-order modes in a symmetrical metal-cladding optical waveguide," *Appl. Phys. Lett.* **85**(20), 4579–4581 (2004).
19. J. H. Gu, G. Chen, Z. Q. Cao, and Q. S. Shen, "An intensity measurement refractometer based on a symmetric metal-clad waveguide structure," *J. Phys. D Appl. Phys.* **41**(18), 185105 (2008).
20. F. Chen, Z. Q. Cao, Q. S. Shen, X. X. Deng, B. M. Duan, W. Yuan, M. H. Sang, and S. Q. Wang, "Picometer displacement sensing using the ultrahigh-order modes in a submillimeter scale optical waveguide," *Opt. Express* **13**(25), 10061–10065 (2005).
21. W. P. Chen and J. M. Chen, "Use of surface plasma waves for determination of the thickness and optical constants of thin metallic films," *J. Opt. Soc. Am.* **71**(2), 189–191 (1981).
22. K. K. Li, Y. Lu, and Q. Wang, "Electro-optic ceramic material and device," U.S. patent 6, 890, 874B1 (2005).
23. M. Cuniot-Ponsard, J. M. Desvignes, A. Bellemain, and F. Bridou, "Simultaneous characterization of the electro-optic, converse-piezoelectric, and electroabsorptive effects in epitaxial $(\text{Sr}, \text{Ba})\text{Nb}_2\text{O}_6$ thin films," *J. Appl. Phys.* **109**(1), 014107 (2011).
24. K. Kurihara and K. Suzuki, "Theoretical understanding of an absorption-based surface plasmon resonance sensor based on Kretschmann's theory," *Anal. Chem.* **74**(3), 696–701 (2002).

1. Introduction

The development of new optical materials with large EO and CPE coefficients is currently of great interest because of the possibility to further minimize device size and reduce operation voltage [1–8]. Although the lanthanum-modified lead zirconate titanate (PLZT) [1] transparent ceramics exhibits much higher EO and CPE effect than that of LiNbO_3 crystal, its significant electric hysteresis [2] is unsuitable to build the precision apparatuses. Fortunately, the newly presented $(1-x)\text{Pb}(\text{Mg}_{1/3}\text{Nb}_{2/3}\text{Nb}_{2/3})\text{O}_3$ - $x\text{PbTiO}_3$ (PMN-PT) ceramics [3], which is transparent from 500 to 7000 nm of the light wavelength, effectively resolves the issues of hysteresis and possesses a morphotropic phase boundary (MPB) [4,5] between the tetragonal and rhombohedral phases. Its anomalously high EO and CPE properties around the MPB are understood as a result of enhanced polarizability arising from the coupling between the two above-mentioned phases [6,7]. Moreover, no consideration of the crystalline orientation is required [8], as PMN-PT is polycrystalline and polarization independent. Consequently, the PMN-PT transparent ceramics offers promise of widespread applications in the optical communication system, such as optical limiter [9], polarization controller [10] and optical switch [11,12], etc.

Despite the continuous fundamental investigations and extensive utilizations, the values of EO and CPE coefficients of PMN-PT have not been completely known. These complete properties could lay the groundwork for the reliable simulation packages which makes the device design process more efficient. EO coefficients can be determined by one-beam-ellipsometric technique [13,14] for measuring the induced phase retardation between two orthogonal plane-polarized lights and by two-beam-interferometric arrangements [15], such as Mach-Zehnder and Michelson interferometers, for measuring the interference between two parallel plane-polarized lights. On the other hand, the CPE coefficients are always determined from the resonance frequencies by the IEEE standard technique [16]. Diverse as measurement techniques are, they can be characterized by one common shortage, namely involving only one effect. However, when an electric field is applied to PMN-PT ceramics, the changes in the optical path length consists of both the change in refractive index (RI) due to EO effect and the change in sample thickness resulting from the CPE effect. Therefore, it is highly expected that a simple method is capable of measuring the EO and CPE coefficients of PMN-PT ceramics simultaneously.

Recently, it is well established that the ultrahigh-order modes excited in the symmetrical metal-cladding waveguide (SMCW) [17–20] are highly sensitive to the changes of RI and thickness within the guiding layer. That is because the light field confined in the guiding layer is not in the form of evanescent wave but oscillating wave. The SMCW-based oscillating wave sensor has been achieved experimentally, yielding a detection limitation of 8.8×10^{-8} in RI units [18] and 3.3 pm in thickness [19]. In this paper, we take advantage of the high sensitivity of the ultra-high order modes in response to the change of the guiding layer parameters and the small separation between two adjacent ultra-high order modes to establish a correlation between EO and CPE coefficients of PMN-PT ceramics. With this correlation and the measurement of the effective RI change to the applied voltage, the quadratic EO and CPE coefficients of PMN-PT ceramics are obtained simultaneously.

2. Structure and principle

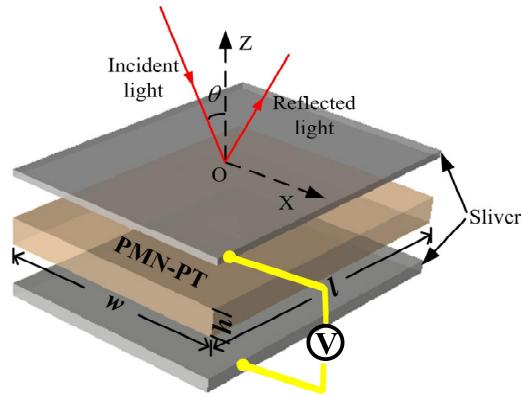


Fig. 1. Structure of SMCW. The PMN-PT ceramics is sandwiched by two sliver films which act as the cladding and the electrodes to supply electric field.

The schematic layout of the SMCW for simultaneously measuring EO and CPE coefficients of PMN-PT ceramics (provided by Boston Applied Technology Inc.) is illustrated in Fig. 1. A thin sliver film and a relative thick sliver film are deposited on the top and bottom side of the PMN-PT ceramics by the thermal evaporation technology, and functioned as the coupling layer and substrate, respectively. Moreover, these two sliver films are also employed as electrodes to supply electrical field and thus the optical properties of the guiding layer can be electrically controlled. From top to bottom, the refractive index (dielectric coefficient) and thickness of the SMCW structure are denoted by n_j (ϵ_j), h_j ($j=1,2,3$), respectively.

Because of symmetrical metal cladding, the effective index of guided modes can be in the range of $[0, 1]$, it is uniquely capable to couple light directly from free space into SMCW [17]. Furthermore, owing to the millimeter scale thickness of the guiding layer, the waveguide can accommodate tens of thousand modes. Dispersion equation of the m th ultra-high order mode ($m > 1000$) can then be simply approximated as [18]

$$\kappa_2^m h_2 = m\pi, \quad m = 0, 1, 2, \dots, \quad (1)$$

where $\kappa_2^m = \sqrt{k_0^2 n_2^2 - \beta_m^2}$ is the vertical propagation constant, $k_0 = 2\pi/\lambda$ is the wavenumber with light wavelength λ in free space, and $\beta_m = k_0 N_m$ is the transverse propagation constant with the effective index N_m of the guided modes. The resonance excitation of the guided mode occurs at

$$\beta_m = k_0 n_{\text{air}} \sin \theta_m, \quad (2)$$

where n_{air} represents the RI of the air, θ_m is the incident angle, and m is the mode order. Two typical ultrahigh-order modes (their mode orders are denoted by $m+1$ and m) with small N are shown in Fig. 2. The used calculating parameters are as follows: $n_{\text{air}} = 1.0$, $n_2 = 2.620$, $\varepsilon_1 = \varepsilon_3 = -18.6 + 0.5i$, $h_1 = 39\text{nm}$, $h_2 = 3.0\text{mm}$, $h_3 = 300\text{nm}$ and $\lambda = 632.8\text{nm}$. The RI of PMN-PT ceramics was obtained from the material supplier (provided by Boston Applied Technology Inc.). The thickness and the complex dielectric permittivity of the top silver film are determined by the double-wavelength method [21]. When an electric field is applied, the RI and thickness of PMN-PT ceramics is altered by the EO and CPE effect, and then the synchronous angles (θ_{m+1}, θ_m) of the two ultrahigh-order modes are shifted to a new position (θ'_{m+1}, θ'_m).

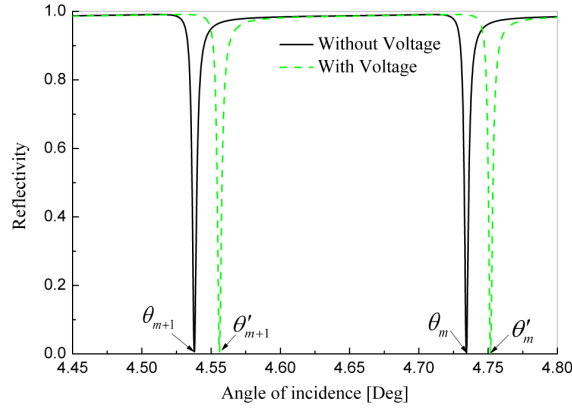


Fig. 2. (Color online) Theoretical variation of synchronous angles in response to the applied voltage.

According to differential principle and Eq. (1), one can obtain the variation of the effective RI as

$$\Delta N = \frac{n_2}{N} \Delta n_2 + \frac{n_2^2 - N^2}{N h_2} \Delta h_2, \quad (3)$$

where Δn_2 and Δh_2 are the electric field-induced changes in the RI and thickness of PMN-PT ceramics, respectively. It is seen that the effective RI of the ultrahigh-order modes, which are excited at very small incident angles, i.e. $N \rightarrow 0$, shows a high sensitivity to Δn_2 and Δh_2 .

The birefringence Δn_2 of an electro-optic material in the presence of an electric field can be described by the equation

$$\Delta n_2 = \Delta n_{20} - \frac{n_2^3}{2} \left[\gamma \left(\frac{V}{h_2} \right) + S \left(\frac{V}{h_2} \right)^2 \right], \quad (4)$$

where Δn_{20} is the birefringence of the material in the absence of an electric field, γ and S is the linear Pockels EO coefficient and the quadratic Kerr EO coefficient, respectively, and V is the applied voltage. Since PMN-PT is optical isotropic in the absence of an electric field [10,22], Δn_{20} and γ are essentially zero. If the incident light is TE polarized, the RI change of the PMN-PT ceramics can be simplified from Eq. (4)

$$\Delta n_2 = -\frac{1}{2} n_2^3 S_{33} \left(\frac{V}{h_2} \right)^2, \quad (5)$$

where S_{33} is a component of the quadratic EO coefficient. For the case of the linear electro-optical ceramics, the similar analysis process can be easily obtained.

The thickness change of the PMN-PT ceramics is expressed as

$$\Delta h_2 = d_{33} h_2 \left(\frac{V}{h_2} \right), \quad (6)$$

where d_{33} is a component of CPE coefficient. By combining Eq. (5) and Eq. (6), the variation of effective RI in Eq. (3) can be rewritten as

$$\Delta N = AV^2 + BV, \quad (7)$$

where

$$\begin{cases} A = -\frac{1}{2} \frac{n_2^4}{N h_2^2} S_{33} \\ B = \frac{n_2^2 - N^2}{N h_2} d_{33} \end{cases} \quad (8)$$

In Eq. (7), n_2 and h_2 are the known quantities, V is the applied electric voltage, effective RI $N = n_{air} \sin \theta$ and ΔN can be detected in the experiment. S_{33} and d_{33} are quantities to be determined. It is clear that Eq. (7) can be solved only if there is a correlation between S_{33} and d_{33} .

Because of the high sensitivity with $N \rightarrow 0$ of the ultra-high order modes and small separation between two adjacent modes, it is possible that exerting a certain critical voltage V^c to shift the synchronous angle of the $(m+1)$ th mode from θ_{m+1} to θ_m which is just that of m th mode in the case of zero applied electric field. The new dispersion equation of the $(m+1)$ th mode under the critical voltage is then expressed by

$$\kappa_2^{m+1} (h_2 + \Delta h_2) = (m+1) \pi, \quad (9)$$

where $\kappa_2^{m+1} = \sqrt{k_0^2 (n_2 + \Delta n_2)^2 - \beta_{m+1}^2}$. On subtracting Eq. (1) from Eq. (9), we obtain

$$(\kappa_2^{m+1} - \kappa_2^m) h_2 + \kappa_2^{m+1} \Delta h_2 = \pi, \quad (10)$$

Since $\beta_{m+1} = \beta_m$ due to $\theta_{m+1} = \theta_m$, and the numerical simulation verifies that Δn_2 and $\frac{\Delta h_2}{h_2}$ are less than 10^{-4} order of magnitude as θ_{m+1} shifted to θ_m . In this case, after neglecting the higher-order small quantities one yields

$$\kappa_2^{m+1} - \kappa_2^m = \frac{n_2 k_0^2 \Delta n_2}{\kappa_2}, \quad (11)$$

By combining Eqs. (5)-(6) and Eqs. (10)-(11), a new correlation between quadratic EO and CPE coefficients can be cast in the form

$$-\frac{k_0^2}{2\kappa_2} n_2^4 h_2 \left(\frac{V^c}{h_2} \right)^2 S_{33} + \kappa_2 h_2 \left(\frac{V^c}{h_2} \right) d_{33} = \pi, \quad (12)$$

where $\Delta n_2 = -\frac{1}{2} n_2^3 S_{33} \left(\frac{V^c}{h_2} \right)^2$ and $\Delta h_2 = d_{33} h_2 \left(\frac{V^c}{h_2} \right)$ are the corresponding changes in the RI and thickness of the PMN-PT ceramics with applied critical voltage V^c .

Substituting Eq. (12) into Eq. (7) and using Eq. (8), the quadratic EO and CPE coefficients can be determined with the detection values of A and B . In order to assure the reliability of the scheme, the obtained results are further checked by fitting the experiment data to the quadratic function Eq. (7).

3. Experiment and discussion

The optical arrangement for simultaneously measuring the EO and CPE coefficients of PMN-PT ceramics based on the SMCW structure is shown in Fig. 3. A polarizer and two apertures with diameters of 1 mm are subsequently placed about 0.5 m apart. An incident light from a He-Ne laser passes through them to be TE polarized and further collimated. We used a PMN-PT ceramics with dimensions of $5.62\text{mm} \times 4.20\text{mm} \times 3.00\text{mm}$ (*length* \times *width* \times *thickness*), which is deposited with two sliver films and firmly mounted on a $\theta/2\theta$ goniometer, and the intensity of the reflected light is detected by a photodiode (PD). A home-made software allows personal computer to control the goniometer and record a series of resonance dips corresponding to the excited guide modes.

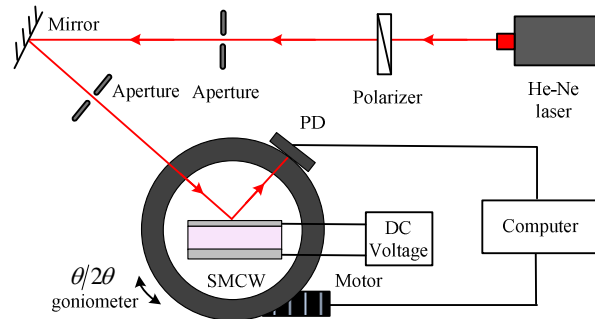


Fig. 3. Experiment arrangement for simultaneously measuring the EO and CPE coefficients of PMN-PT ceramics. PD: photodiode.

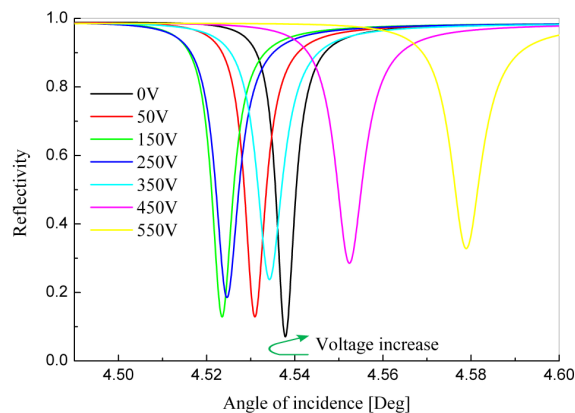


Fig. 4. (Color online) Measured resonance dips as a function of the angle of incidence for various applied voltages.

In the experiment, the angle of incidence is set around one selected ultrahigh-order mode ($\theta = 4.537^\circ$), because the guide mode excited at small angle can offer a higher sensitivity [18]. The measured resonance dip as a function of the angle of incidence for various applied voltages is shown Fig. 4. Because of $\Delta n_2 > 0$ and $\Delta h_2 < 0$ at any exerted voltage, variation of the resonance peak induced by EO and CPE effects partially compensates one another. Under low voltages, the resonance dip shifts to the left side because the contribution of the CPE effect is greater than that of EO effect (i.e. $\Delta N < 0$). As the applied voltages are larger than 400V, the resonance dip shifts to the right side since the contribution of the EO effect in this case is predominated (i.e. $\Delta N > 0$) because the EO effect is a quadratic function of voltage. The critical voltage V^c for the resonance dip of the $(m+1)$ th mode tends to that of the adjacent (m) th mode (under zero-field) is about 900V. By using Eqs. (7)-(8) and Eq. (12), and using Eq. (8), we obtain the quadratic EO coefficient $S_{33} = -2.24 \times 10^{-16} \text{ m}^2/\text{V}^2$ and the CPE coefficient $d_{33} = -96 \text{ pm}/\text{V}$ of PMN-PT ceramics. In Fig. 4 it is found that the minimum reflectance and the FWHM of the resonance dips gradually increase with the increasing applied voltages, it is perhaps in virtue of an electro-absorptive effect in PMN-PT ceramics [23]. That is because the radiative damping and intrinsic damping of the waveguide structure, which are two factors to determine the minimum reflectance and the FWHM of the resonance dips [24], are functions of the extinction coefficient κ of PMN-PT ceramics that can altered by the electro-absorptive effect.

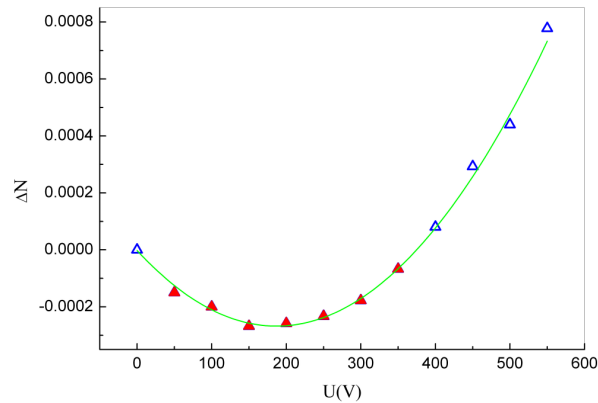


Fig. 5. The variation of effective RI related to various applied voltages. The quadratic curve was obtained by fitting the experiment data to Eq. (6). The red closed triangles and the blue open triangles coresspond to the left and right shift of synchronous angles in Fig. 4, respectively.

The variation of effective RI related to various applied voltages is shown in Fig. 5. It is clear that the negative vaules (red closed triangles) of the variation in effective RI coresspond to the left shift of the resonance peak while positive values (blue open triangles) coresspond to the right shift of the resonance peaks in Fig. 4, respectively. By fitting the experiment data to a quadratic function, the parameters $A = 7.5927 \times 10^{-9}$ and $B = -2.839 \times 10^{-6}$ in Eq. (7) are obtained. By submitting the above parameters into Eq. (6), the same results of the quadratic EO coefficient and the CPE coefficient of PMN-PT ceramics are finally received.

4. Conclusion

In conclusion, a simple method to measure the EO and CPE coefficients of PMN-PT ceramics simultaneously has been described. This method is based on the high sensitivity to the RI and the thickness of the guiding layer of the ultra-high order modes and the small separation between two adjacent ultra-high order modes. By exerting a critical voltage on the PMN-PT

ceramics, a resonance dip can reach the position of the adjacent mode. In this way, we established a correlation between EO and CPE coefficients. Measurement has been performed for a PMN-PT ceramics, and the results are in good agreements with the data obtained by other methods.

Acknowledgments

This work was supported by the National Natural Science Foundation of China (Grant No. 61168002), and opening foundation of the State Key Laboratory of Advanced Optical Communication Systems and Networks (Grant No. 2011GZKF031105).